

A newly developed anesthetic based on a unique chemical core

Noëlie S. Cayla^a, Beza A. Dagne^a, Yun Wu^a, Yao Lu^a, Larry Rodriguez^b, Daryl L. Davies^b, Eric R. Gross^a, Boris D. Heifets^a, M. Frances Davies^{a,c}, M. Bruce MacIver^a, and Edward J. Bertaccini^{a,c,1}

^aDepartment of Anesthesiology, Perioperative and Pain Medicine, Stanford University School of Medicine, Stanford, CA 94305; ^bDepartment of Molecular Pharmacology and Toxicology, University of Southern California School of Pharmacy, Los Angeles, CA 90089; and ^cDepartment of Anesthesia, Palo Alto VA Health Care System, Palo Alto, CA 94304

Edited by Emery N. Brown, Massachusetts General Hospital, Boston, MA, and approved June 19, 2019 (received for review December 28, 2018)

Intravenous anesthetic agents are associated with cardiovascular instability and poorly tolerated in patients with cardiovascular disease, trauma, or acute systemic illness. We hypothesized that a new class of intravenous (IV) anesthetic molecules that is highly selective for the slow type of γ -aminobutyric acid type A receptor (GABA_AR) could have potent anesthetic efficacy with limited cardiovascular effects. Through in silico screening using our GABA_AR model, we identified a class of lead compounds that are *N*-arylpyrrole derivatives. Electrophysiological analyses using both an in vitro expression system and intact rodent hippocampal brain slice recordings demonstrate a GABA_AR-mediated mechanism. In vivo experiments also demonstrate overt anesthetic activity in both tadpoles and rats with a potency slightly greater than that of propofol. Unlike the clinically approved GABAergic anesthetic etomidate, the chemical structure of our *N*-arylpyrrole derivative is devoid of the chemical moieties producing adrenal suppression. Our class of compounds also shows minimal to no suppression of blood pressure, in marked contrast to the hemodynamic effects of propofol. These compounds are derived from chemical structures not previously associated with anesthesia and demonstrate that selective targeting of GABA_AR-slow subtypes may eliminate the hemodynamic side effects associated with conventional IV anesthetics.

anesthesia | drug discovery | mechanism | gamma amino butyric acid receptor

Anesthetics have been successfully administered for over 170 y. Unfortunately, all current IV anesthetic agents have detrimental side effects, most notably hemodynamic suppression. It is for this reason that we have ventured to design a class of anesthetics that are devoid of such side effects. Our drug design strategy has been based on the recent advances in computational chemistry which lead to a validated model of the gamma amino butyric acid type A receptor GABA_AR (1, 2). Sophisticated molecular computations, previously only available via supercomputing facilities, can now be achieved with advanced desktop workstations. Software development has taken full advantage of high-end 3D visualization as well as highly parallelized computational algorithms for efficient drug screening methodologies. Along with these advances, our understanding of the molecular substrates for conscious states has also progressed in the form of robust models of a GABA_AR ligand-gated ion channel that is known to mediate important anesthetic actions (3). The concept presented here is to leverage such advances in computational capabilities for high throughput in silico screening to perform efficient lead compound refinement and drug design using our newly developed molecular models of the GABA_AR. Our current work has now identified a class of lead compounds that demonstrate overt anesthetic activity in mammals via a GABA_AR mechanism, while producing minimal to no hemodynamic perturbations. This is a marked improvement over the detrimental effects of propofol on blood pressure, the current gold standard of IV anesthetics.

After modeling the unwanted interaction of etomidate with the enzyme 11- β -hydroxylase, believed to cause adrenal suppression (4, 5) we investigated alternatives suggested by previous findings (6–9), and then designed a unique molecular core in silico. A selection of 11 lead compounds were identified as similar to our newly designed core after high-throughput structural screening. Subsequent molecular docking was performed using our current GABA_AR model. These compounds were then tested on acutely dissected rodent brain slices and *Xenopus* oocytes for validation of GABA_AR-mediated inhibition mechanisms and in vivo in tadpoles for loss-of-righting reflex (LORR). The most potent compound of the series (BB) was then tested for both LORR and hemodynamic effects in rats.

Results

Molecular Modeling of the 11- β -Hydroxylase Enzyme and Its Interactions with Etomidate, Carboetomidate, 1n, and Carbo-1n. Anesthetics interact with many functional proteins, resulting in a variety of important side effects. In particular, etomidate has a strong inhibitory effect on a critical enzyme for steroid biosynthesis, 11- β -hydroxylase (11CYPB). This effect can result in considerable adrenocortical suppression. A deeper understanding of this process requires a more thorough molecular description of the relevant drug–protein

Significance

The 4 intravenous anesthetics currently in clinical use are associated with undesirable side effects such as lower blood pressure. These agents are poorly tolerated in young and elderly patients, limiting their use and increasing their risks. Additionally, etomidate, an anesthetic that achieves stable cardiovascular conditions, causes significant adrenal suppression by inhibiting steroid biosynthesis. Even though the exact mechanisms of anesthesia remain unknown, a significant component appears to be mediated by γ -aminobutyric acid type A receptors (GABA_ARs). By targeting an anesthetic binding site in these receptors, we are designing anesthetics with reduced side effects. A unique agent based on this design is now shown to be potent and selective for GABA_A-slow receptors and produces anesthesia with minimal hemodynamic side effects.

Author contributions: D.L.D., E.R.G., B.D.H., M.B.M., and E.J.B. designed research; N.S.C., B.A.D., Y.W., Y.L., L.R., D.L.D., E.R.G., B.D.H., M.F.D., and E.J.B. performed research; E.J.B. contributed new reagents/analytic tools; N.S.C., L.R., B.D.H., M.F.D., and E.J.B. analyzed data; and N.S.C., L.R., B.D.H., M.F.D., M.B.M., and E.J.B. wrote the paper.

Conflict of interest statement: E.J.B. and M.F.D. are coinventors on the patent WO 2016/061538 A1 “Novel Methods, Compounds, and Compositions for Anesthesia” and they, their department, and their institution could receive royalties related to the development of these new anesthetic agents.

This article is a PNAS Direct Submission.

Published under the PNAS license.

¹To whom correspondence may be addressed. Email: edwardb@stanford.edu.

This article contains supporting information online at www.pnas.org/lookup/suppl/doi:10.1073/pnas.1822076116/-DCSupplemental.

Published online July 15, 2019.

interactions. While the exact molecular structure of all forms of 11CYPB remain unknown, significant progress has been made toward understanding their interactions with anesthetics using molecular modeling as noted here. We therefore built a molecular model of 11CYPB and performed in silico docking analyses of several important ligands to its binding site. The basic local alignment search tool (BLAST) derived scores and CLUSTALW profile-to-profile alignment demonstrated reasonable sequence similarity between 11CYPB and the modeling templates. The model of the 11CYPB has a cavity of $\sim 810 \text{ \AA}^3$ and can readily accommodate a steroid analog. Within the lowest frequency, highest amplitude natural harmonic motions of this channel, normal mode analyses suggest that this cavity is located in a region of reasonable flexibility, which could be critical to a “clamshell-like” opening motion for binding site access. Etomidate, carboetomidate, 1n, and carbo-1n docking reveal a potentially reversible carbonyl interaction with the heme iron; however, only etomidate and 1n clearly show an imidazole nitrogen available for strong coordinate bond interaction with the heme iron (*SI Appendix, Fig. S1*). Therefore, it is predicted that carbo-1n and its relatives derived from the similarity search of the Chemical Abstracts database should not significantly inhibit steroid biosynthesis. This result is consistent with the already experimentally derived validation of the loss of adrenal suppression via the lack of 11CYPB suppression shown by Raines et al. with their conversion of an imidazole to a pyrrole in the making of carboetomidate (9).

In Silico Modeling and High-Throughput Screening Lead to a Selection of Compounds Whose Relative Potencies Are Predicted via Molecular Docking to the GABA_AR. In our previous work, docking of the initial propofol derivative series to the region bound by specific anesthetic binding residues showed strong linear correlation with the experimentally derived EC₅₀ for GABA_AR potentiation as

suggested by an R^2 of 0.85 (1, 2). CDocker scoring was also validated by the results of the control compounds with known inactivity at the GABA_AR. In the current work (Fig. 1), additional docking of the members from the substituted 1,2-diphenylimidazole series from Asproni et al. (6) which includes 1n (also known as TG41 in their other work) showed a strong correlation of a slightly different docking score, the CDocker Interaction Energy (CDIE) score, with experimentally derived GABA_AR potentiation EC₅₀. This correlation not only spanned the previously studied propofol-like compounds, but included several of the etomidate-like derivatives, as well as carbo-1n, in addition to the 11 compounds similar to carbo-1n. In particular, one experimental compound, BB, appears to be about an order of magnitude less potent than 1n or TG41 which has a known EC₅₀ for GABA_AR potentiation of 0.19 μM . However, the actual approximate EC₅₀ for GABA_AR potentiation of BB appears to be around 0.5 μM in both patch clamp studies as well as tadpoles as noted below.

LORR Assays Confirm Anesthetic Activity and Determine a Lead Compound. Seven of the 11 compounds in Fig. 2 that were tested for LORR in tadpoles had potencies less than 40 μM (Fig. 3A). Compounds AA and BB showed potent anesthetic activities as predicted by the in silico modeling. The EC₅₀ measurements in the tadpoles (Fig. 3B and C) showed that BB was more potent than AA (0.49 μM for BB, and 1.5 μM for AA). The slope of the BB dose-response curves were very steep. All tadpoles recovered a robust LORR once placed into a water bath without drug. After this second round of screening, BB was chosen as the lead compound. Its anesthetic activity was subsequently tested in rats via LORR assays. Intravenous injection of the vehicle controls alone did not produce any behavioral effects. The ED₅₀ value for this compound in rats was determined to be 4.3 mg/kg

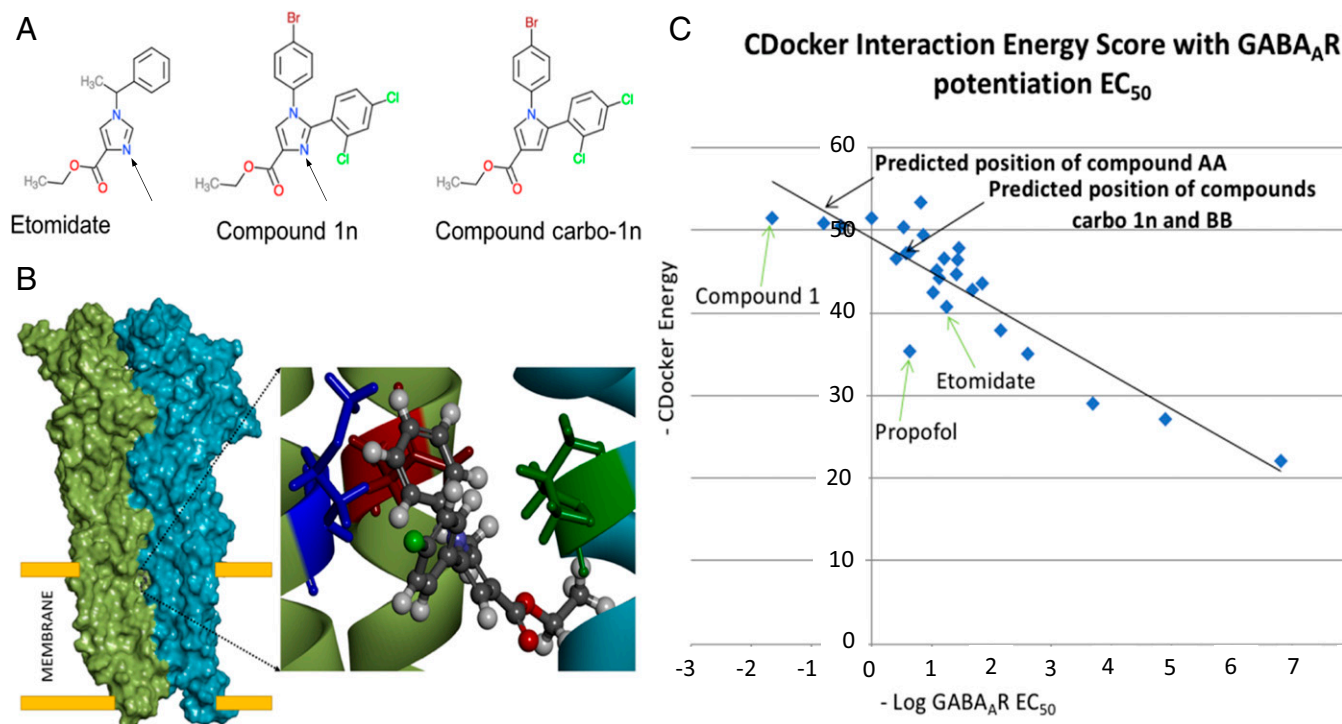


Fig. 1. In A, the arrow points to the nitrogen atom of etomidate involved in complexing with the heme iron in the enzyme, 11- β -hydroxylase, thereby inhibiting corticosteroid biosynthesis. A class of IV anesthetic was developed using a chemical core by converting the free nitrogen in the imidazole ring of 1n to a pyrrole ring shown in carbo-1n. The molecular model (B) shows an anesthetic binding site within the transmembrane component of the GABA_AR and the computationally docked structure of carbo-1n. C shows the docking scores of multiple compounds from the series involving 1n, propofol, and etomidate. These served as reference agents to approximate the GABA_AR docking scores of carbo-1n and its derivatives, notably AA and BB (see Fig. 2 for their structures). Their predicted positions noted by arrows predicted a potency making them worthy of subsequent experimental evaluation.

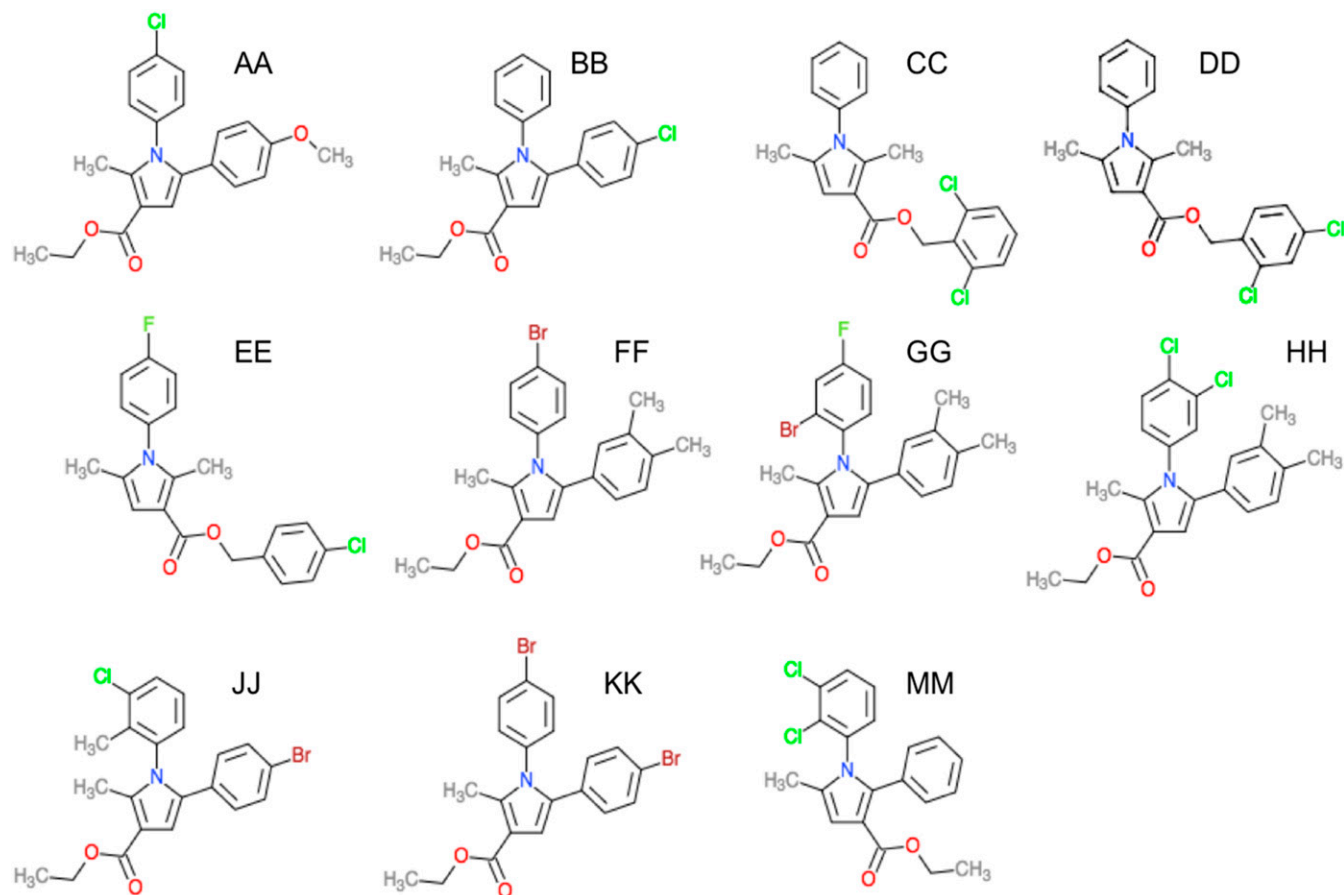


Fig. 2. Structures of the 11 compounds derived from the *in silico* structural similarity search for compounds resembling carbo-1n since the latter did not exist.

(95% confidence limits 3.9 to 4.7). Rodents ($n = 4$) injected with 8 mg/kg BB lost their righting reflex (nearly twice ED_{50}) at an average time of 2.0 ± 0.41 min and then recovered after an average time of 32 ± 1.9 min. They showed neither grossly abnormal behavioral effects nor any signs of toxicity.

Electrophysiology Recordings Show Evidence of GABA_AR-Mediated Inhibition. Acute hippocampal brain slices preserve major elements of synaptic and circuit organization observed *in vivo* while allowing for detailed electrophysiological investigation (10). We performed field recordings in the CA1 region, measuring population spikes evoked by paired electrical stimuli of afferents in the stratum radiatum, where the timing between the first and second pulse (100 ms) is optimized to test effects on GABA_AR-slow-mediated inhibition, as opposed to effects on GABA_AR-fast-mediated inhibition, measured using the first stimulus. The results shown in Fig. 4 demonstrate that etomidate and BB acted specifically through GABA_AR-slow receptors, since only the second pulse responses were depressed in experiments of paired-pulse inhibition. Propofol had additional effects mediated by GABA_AR-fast and tonic receptors (11, 12), since effects on both first and second pulse responses were produced (13). The effects of all agents were fully reversed by picrotoxin, a chloride channel blocker that acts specifically on GABA_ARs (*SI Appendix, Fig. S2*). These results confirmed that BB produced a reversible enhancement of GABA_AR-slow-mediated inhibition, which was significantly more selective than propofol. The latter, in contrast, clearly enhanced other forms of GABA_AR-mediated inhibition by depressing both first and second pulse responses. Additionally, there was no effect of flumazenil on the BB response.

To directly measure BB's effect on GABA_AR-mediated currents in an intact tissue preparation, we performed whole-cell voltage-clamp recording from CA1 pyramidal cells in mice. Inhibitory postsynaptic currents (IPSCs) were pharmacologically isolated by the continuous perfusion of artificial cerebrospinal fluid (ACSF) containing NMDA and AMPA/Kainate receptor antagonists (25 μ M d-APV and 10 μ M NBQX), such that the resulting evoked current was entirely GABA_AR mediated. GABA release and subsequent IPSCs were evoked by electrically stimulating afferent fibers in the stratum radiatum of the CA1 region, and IPSCs were recorded in the CA1 stratum pyramidale (Fig. 5A). This stimulation protocol is known to preferentially activate GABA_AR-slow inhibitory synapses (14). Decay constants and amplitude of the evoked IPSCs were monitored over time (Fig. 5B–D), in addition to standard measures of whole-cell recording quality, i.e., series and input resistance (Fig. 5E and F). A brief, 10-min perfusion of 40 μ M BB dramatically slowed the decay of evoked IPSCs and produced a modest enhancement of IPSC amplitude. Notably, the vehicle did not have any effect on these measures. Changes in the quality of the pipette seal or changes in the cellular input resistance could not account for the observed slowing of IPSCs with BB (Fig. 5E and F). The IPSC prolongation was substantial enough that currents which typically decayed to baseline in less than 50 ms extended to 100's of milliseconds in the presence of BB. The relatively selective effect on IPSC decay, versus amplitude, mirrors our finding that population spike pairs elicited at a 100-ms interval predominantly demonstrated a reduced second spike amplitude, without a notable effect on the first population spike amplitude.

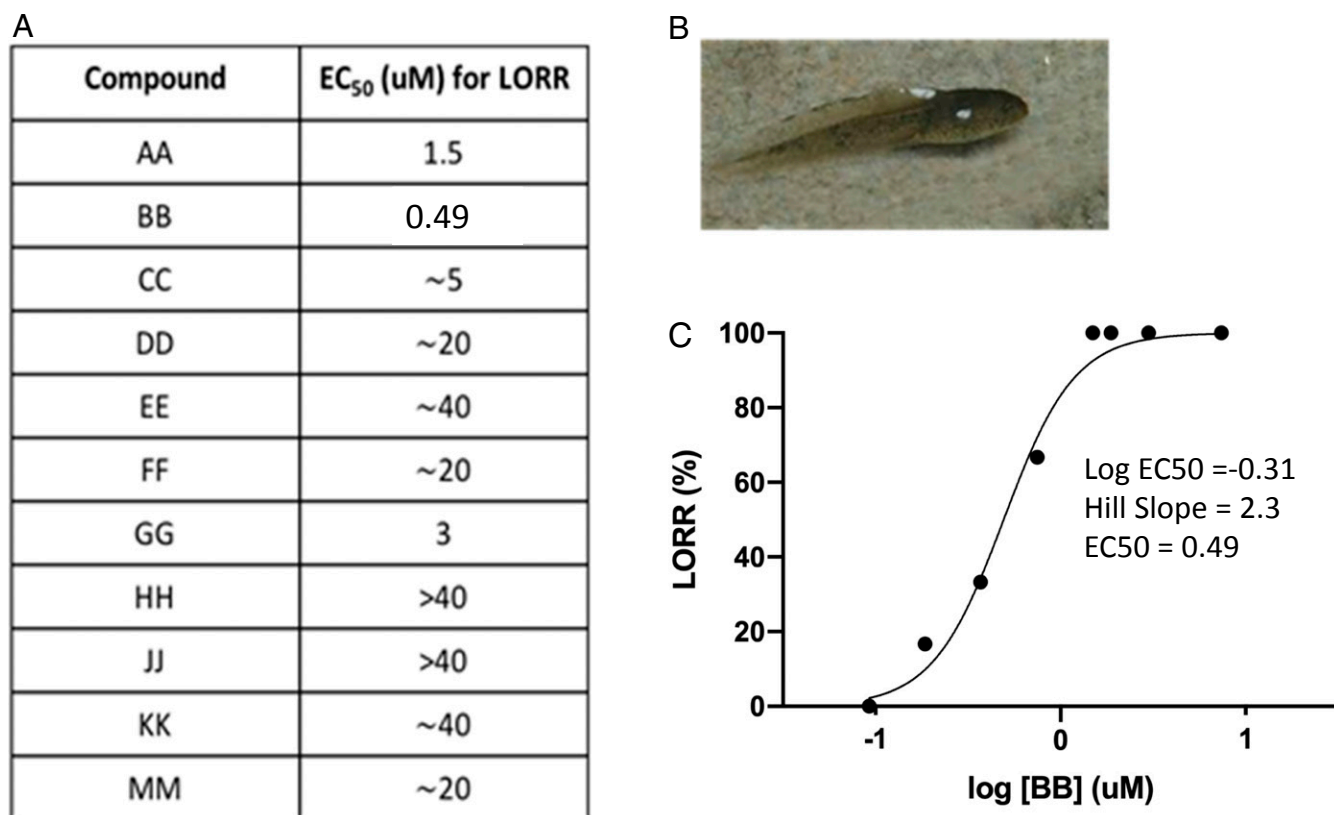


Fig. 3. The EC₅₀ concentration for LORR for each compound (A) in bullfrog tadpoles (B) narrowed down the selection of 11 molecules suggested during the high-throughput screening stage to 1 lead compound. The most potent compound appeared to be BB (EC₅₀ = 0.49 μ M) (C) which was chosen for the rest of the experiments.

To allow a more detailed view of effects on GABA_AR-mediated currents, we tested BB on α 5 containing GABA_ARs expressed in *Xenopus* oocytes. α 5 containing GABA_ARs is known to contribute to both GABA_AR-slow and tonic currents in CA1 pyramidal neurons (14–16). Fig. 6 illustrates the GABA concentration response curve for α 5 β 3 γ 2 GABA_ARs and demonstrated an EC₅₀ of $6.6 \pm 0.7 \mu$ M and EC₂₀ of $3.2 \pm 0.3 \mu$ M (Fig. 6A). BB robustly potentiated GABA-induced currents in a concentration-dependent manner, with an EC₅₀ for GABA EC₂₀ current potentiation of $0.57 \pm 0.17 \mu$ M, very similar to the EC₅₀ for the LORR in tadpoles (Fig. 6B).

In Vivo Hemodynamic Measures Demonstrate a Stable Cardiovascular Profile. The hemodynamic profiles for both BB and propofol were measured in rats and compared in Fig. 7. The ED₅₀ dose of BB for LORR was 4.34 mg/kg (Fig. 7A). This is in comparison with the published ED₅₀ for propofol of 5.13 mg/kg (17). Propofol readily produces a $50 \pm 20\%$ decrease in systolic (Fig. 7B) and diastolic (Fig. 7D) arterial blood pressure after a single IV bolus of 10.0 mg/kg (a typical anesthetic induction dose), while with BB, the values remain stable even at 20 mg/kg, a dose which is over 4 \times the ED₅₀ required for LORR. Heart rate was not sensitive to either drug (Fig. 7C).

In Vivo Corticosteroid Assays Demonstrate a Stable Adrenal Profile. In silico calculations for our compounds predicted the lack of interaction with the heme iron in 11- β -hydroxylase and therefore an inability to suppress adrenal synthesis. This was experimentally tested by determining the effects of BB on corticosterone levels stimulated with ACTH_{1–24} (0.5 mg/kg IV). The baseline levels of corticosterone before any drug was given were similar in

both control vehicle and BB groups. After stimulation with ACTH and administration of either vehicle or BB, there was no difference in the stimulated corticosterone levels between control animals and those receiving BB (Fig. 8A), as well as no difference between groups in the change of stimulated corticosterone levels from baseline (Fig. 8B). Animals receiving either vehicle or BB both produced a marked increase in stimulated corticosterone levels from baseline ($P = 0.0001$, Fig. 8A) in response to ACTH. It should be noted that using the same protocol Wang et al. (18) found that etomidate caused an almost complete suppression of corticosterone synthesis.

Discussion

The drug profiles and dangerous side effects of the currently available IV anesthetic agents are many, especially among infants and the aging geriatric population. Proportionately, the fastest growing segment of the population are octogenarians and older, a group of people who now use the majority of the healthcare dollars and are in need of increasing surgical and anesthetic care. Even among an otherwise healthy population, conditions can arise that render any patient acutely unstable, such as in trauma and battlefield arenas. Therefore, there is significant clinical pressure as well as market opportunity to develop new anesthetics.

There are currently 4 main IV and 3 primary inhalational anesthetic agents in common clinical use. Each of these agents is associated with an entire spectrum of undesirable side effects, most of which result in lower systemic blood pressure (19). This side effect is poorly tolerated in very young children who possess immature cardiovascular compensatory mechanisms, as well as in the elderly with confounding comorbidities and otherwise

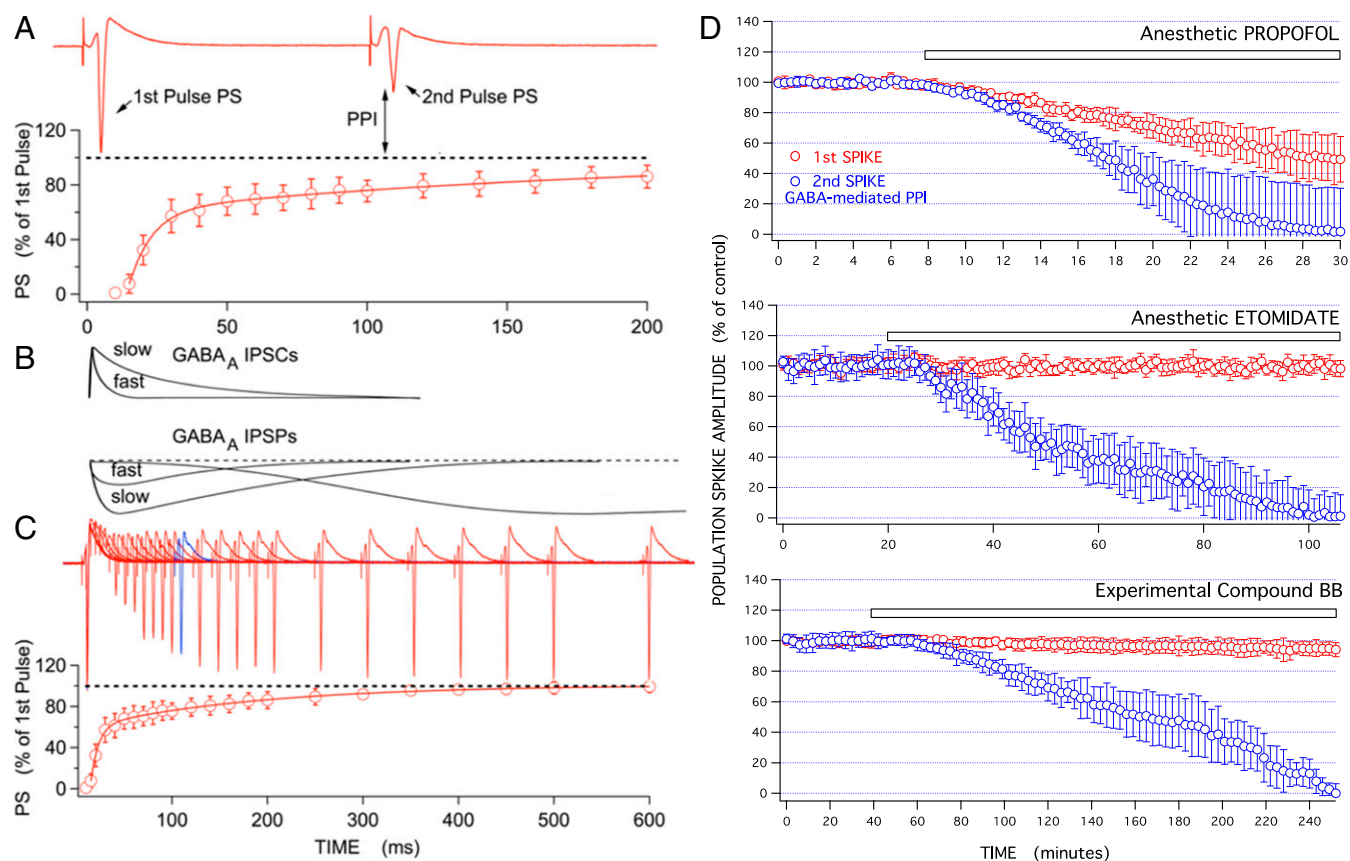


Fig. 4. (A) Paired-pulse population spike responses were recorded from hippocampal rat brain slices to measure anesthetic effects on tonic currents. Each symbol represents the mean \pm SD for $n = 5$. (B and C) Fast (first pulse) and slow (second pulse) inhibitory pathways in the CA1 area neural circuit. By 100 ms it is too late to have the involvement of fast synapses, but ideal for following the time course of slow synapses. Each symbol represents the mean \pm SD for $n = 5$ in C. Increased stimulation engages inhibitory circuitry, resulting in the paired pulse inhibition (PPI) measure between the first and second population spikes (PSs). Effects on tonic inhibition would contribute equally to both responses. (D) Population spike depression time course produced by propofol, etomidate, and BB showed significant differences in GABA_AR involvement for first (in red) vs. second pulse responses (in blue). Minutes (min) are post-drug application. Each symbol represents the mean \pm SD for $n = 10$ propofol; $n = 5$ etomidate; $n = 7$ BB. In D, the following statistical comparisons were made: first pulse propofol (30 min) vs. first pulse etomidate (40 min) $P < 0.005$; first pulse propofol (30 min) vs. first pulse BB (120 min) $P < 0.001$. For second pulse responses there were no significant differences between drugs for the depressions produced, since all produced 100% depression.

exhausted compensatory mechanisms. Each of these agents has additional unique detriments. In particular, etomidate is the agent which comes closest to achieving ideal cardiovascular preservation while inducing dose-dependent alterations in consciousness. However, this stability comes at the expense of clinically significant adrenal suppression via inhibited steroid biosynthesis. Propofol has gained wide popularity, but produces profound hypotension and, most notably in the very young, has also been associated with the propofol infusion syndrome characterized by extreme metabolic acidosis and death.

Several groups have developed compounds with similar overall shape to our lead class and that have effects at the GABA_AR. However, each has marked variation in their individual atomic constituents that not only make them chemically distinct, but are also characterized by variable physicochemical properties and methods of syntheses. For instance, the aryl pyrazoles described by Mascia et al. have a 5-membered ring at their core in which are adjacent nitrogens, variable halogen substitutions on the attached phenyl rings, and an amide-linked substituent (20). This is a class that is similar to many known cannabinoid receptor antagonists, which is also discussed in their work. The imidazole series presented by Asproni et al., while initially developed for other purposes, demonstrated several compounds with potent GABA_AR activity (6). However, as alluded to above, they contain a central 5-membered imidazole ring, with variable attached

phenyl ring substitutions and an ester group also with variable substitutions. Further, both the pyrazoles and the imidazoles contain a nitrogen with a free electron pair, making them susceptible to interaction with the heme iron of 11CYPB, therefore having the potential to produce adrenal suppression like etomidate.

In this study, we implemented state-of-the-art molecular computations, previously only available via supercomputing facilities that combine advanced molecular modeling and 3D visualization with highly parallelized computational algorithms for efficient drug screening in an effort to design the next generation of safer IV anesthetic. We iteratively leveraged this technology to identify leads based on our validated models of the anesthetic binding site within the GABA_AR for subsequent *in vitro* and *in vivo* measures of potency and physiologic effects. A successful computational selection of 11 potential anesthetic agents with the desired pharmacologic characteristics allowed the identification of a lead compound, BB, with a safer and more potent profile exhibited during *in vitro* and *in vivo* studies of anesthetic efficacy. The concept presented here demonstrates the advantages of high-throughput *in silico* screening (via structural screening and ligand-receptor docking methodologies) in an effort to better perform efficient lead refinement and drug design using current molecular models of the GABA_AR. Mechanistically, a class of anesthetic compounds has been identified that is devoid of the moiety known to produce adrenal suppression in etomidate.

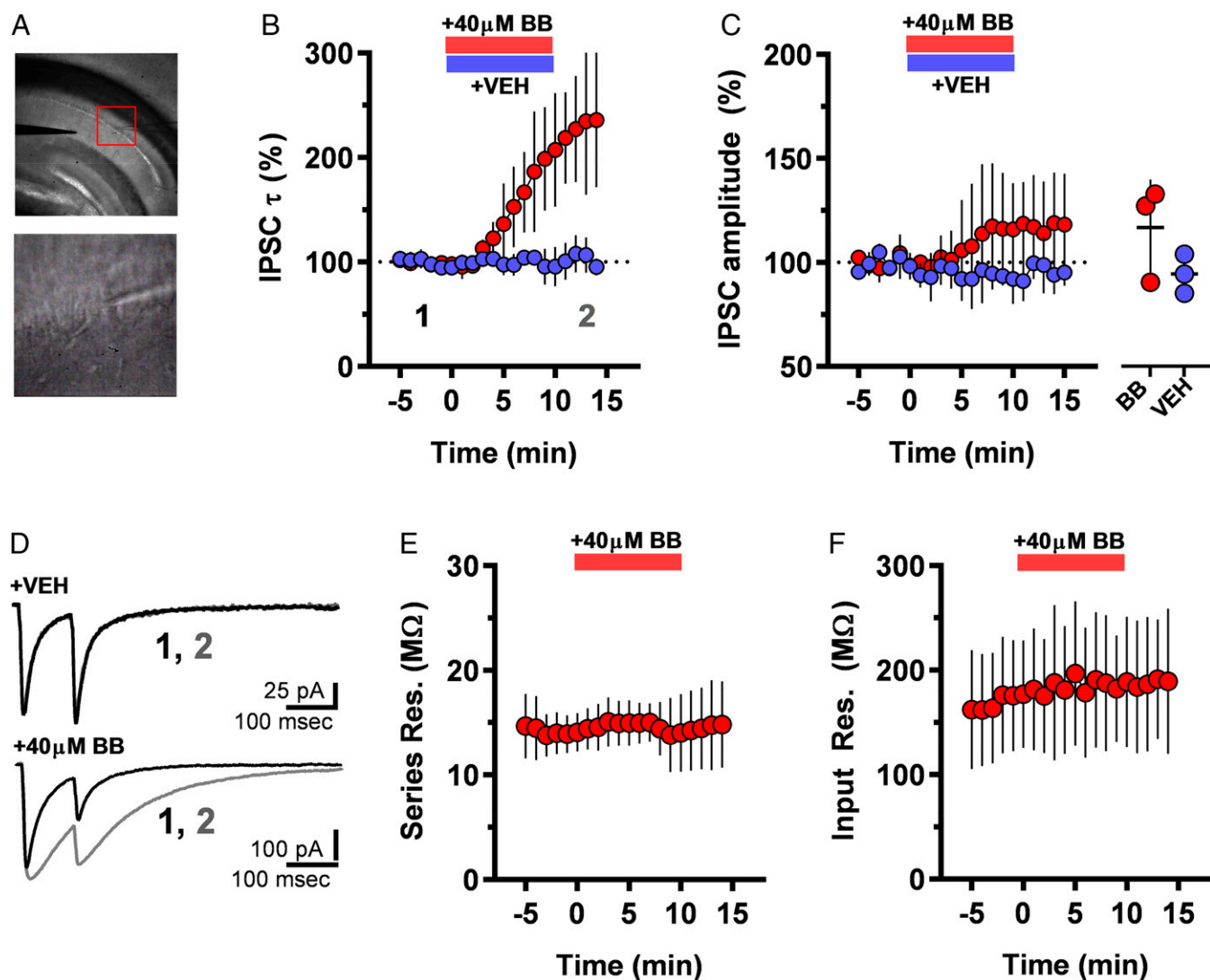


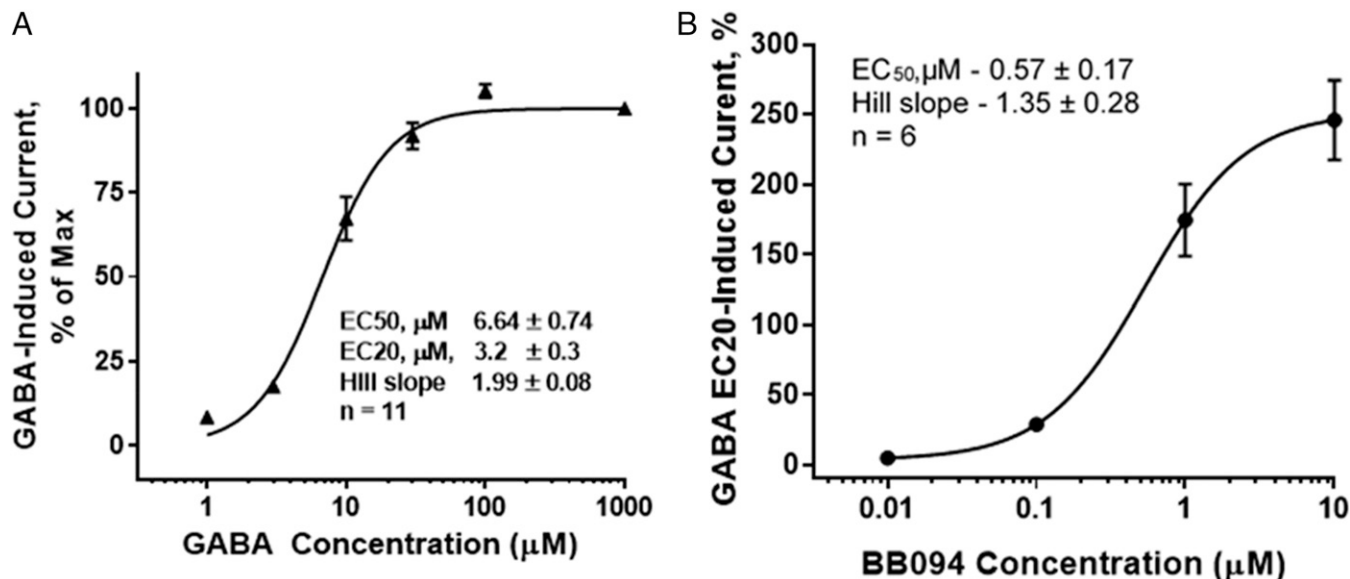
Fig. 5. Compound BB dramatically prolongs GABA_A-mediated IPSCs. (A) Configuration for electrically evoking and recording IPSCs. (A, Top) Photomicrograph (10×) of a transverse hippocampal slice from mouse. Monopolar stainless steel stimulating electrode is placed in the stratum radiatum, and recording pipette in the stratum pyramidale, of hippocampal area CA1. Red box indicates field of magnified image (60×) at Bottom, in which the recording pipette is attached to a pyramidal cell. (B) IPSC duration, measured by the monoexponential decay constant, τ , is significantly prolonged in the presence of BB, but not vehicle (VEH). VEH or 40 μ M BB compound was perfused into the recording chamber from time 0 until time 10. Points 1 and 2 indicate times where representative evoked IPSC traces (D) were taken. At Right of graph, the % change of τ versus predrug baseline is shown for both BB and VEH conditions. Individual cell data and group mean \pm SD are plotted for the epoch between 10 and 15 min after BB/VEH application. (C) In the same set of experiments shown in B, BB, but not VEH, modestly enhanced IPSC amplitude. Changes of IPSC amplitude versus baseline are again shown at Right of graph for individual cells and group mean \pm SD. (D) Representative IPSC traces before and after application of VEH or BB (time points indicated in B). (E and F) BB did not change parameter recording quality, as measured by resistance of the recording electrode in series with the recorded cell (series resistance, E) and the cell's global resistance to alterations in membrane potential (input resistance, F), indicating little or no effect on tonic GABA_AR currents were produced.

Subsequent experiments were thereby made more efficient and limited in scope to confirm its anesthetic efficacy in mammals.

It was particularly interesting that BB exhibited a selective depression of the second pulse of a pair of stimuli used to test for effects on GABA_A-slow IPSCs, since GABA_A-fast responses decay long before the 100-ms interval used for the second test pulse. BB shared this selective effect with etomidate, but not with propofol. Propofol depressed both first and second pulse responses, indicating direct effects on both GABA_A-fast and -slow forms of inhibition, as well as tonic GABA_ARs that contribute to the first pulse depression observed (12). Propofol shares this first pulse depression with volatile anesthetics and barbiturates that also produce hemodynamic and respiratory depression (11). This suggests that nonselective actions on tonic

and fast GABA_ARs could contribute to the unwanted hemodynamic side effects, while the common action of enhanced GABA_A-slow inhibition is needed for anesthesia.

In conclusion, our methodologies of *in silico* screening and prediction of compounds that bind to our validated model of the GABA_AR have now identified a class of lead compounds that demonstrate overt anesthetic activity in both tadpoles and rats with a potency greater than that of propofol, the current IV anesthetic standard. These structures are devoid of the chemical moieties known to produce adrenal suppression, a serious side effect of the other commonly used anesthetic, etomidate. Of even greater importance is the fact that BB, the lead representative of this class of compounds, shows minimal to no suppression of blood pressure, in stark contrast to the deleterious hemodynamic



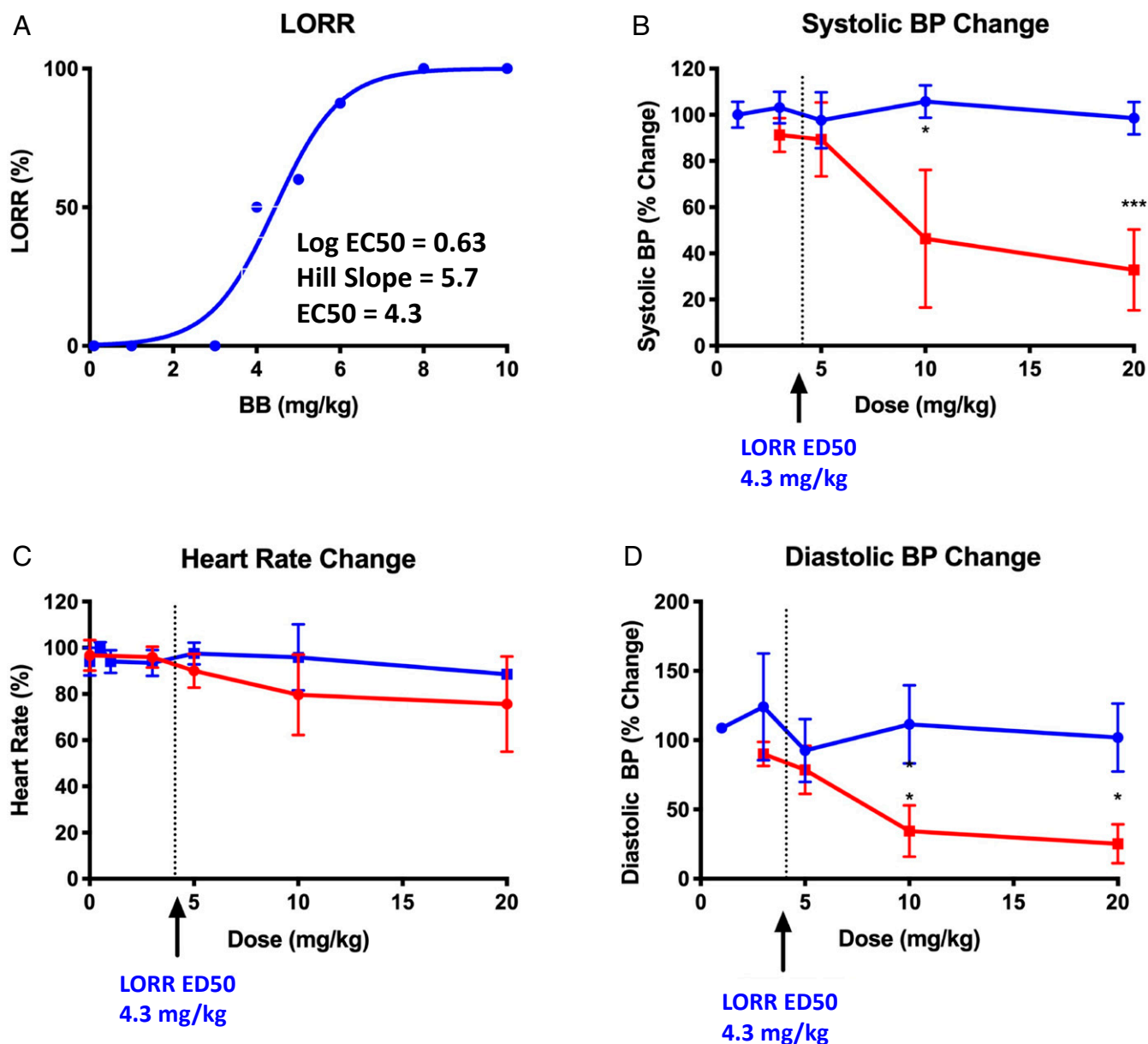
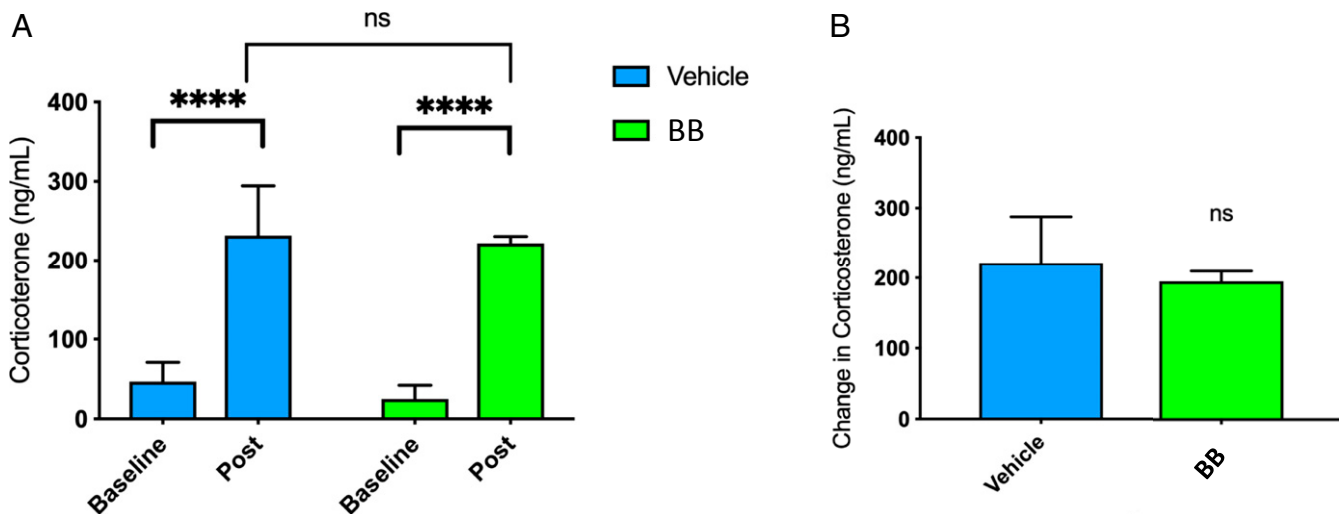


Fig. 7. (A) The dose-response curve for LORR in rats due to IV-administered BB (closed blue circles) showing anesthetic-induced LORR having an ED₅₀ of 4.3 mg/kg. (B) BB had no effect on systolic blood pressure up to 20 mg/kg, whereas IV administration of propofol (closed red squares) significantly reduced systolic blood pressure ($n = 5$, $P < 0.01$) at 20 mg/kg; both have minimal effects on (C) heart rate. (D) The diastolic blood pressure was also suppressed compared with propofol ($n = 5$, $P < 0.05$ at both 10 mg/kg and 20 mg/kg). Error bars refer to SEs from the mean. The blood pressure and heart rates were recorded at 3 min after initiation of the drug injection.

density functional theory (30) and a Perdew–Burke–Ernzerhof functional, while the remainder of the complex was treated with a CHARMM molecular mechanics forcefield (31). Molecular dockings of etomidate and carboetomidate stereoisomers, as well as the 1n and carbo-1n compounds, were performed with the CDocker algorithm as noted above.

Loss-of-Righting Reflex in Tadpoles. Early prelimb-bud stage *Rana catesbeiana* tadpoles (5 per 50-mL beaker) were placed in room temperature oxygenated water buffered with 2.5 mM Tris-HCl buffer (pH = 7.4) and containing a concentration of test compound ranging from 0.1 μ M to 100 μ M. Tadpoles were manually tipped every 5 min with a steel spatula or stream of water and assessed for their ability to maintain righting reflex response until 120 min had elapsed. Tadpoles were deemed to have attained LORR if they failed to right themselves within 5 s after either spontaneous self-turning or being manually turned over on their back. At the end of each study, tadpoles were transferred to fresh water to assess whether the anesthetic action was reversible.

***Xenopus laevis* Oocyte Preparation and Electrophysiology.** For cDNA injections, stage 4 to 5 *Xenopus laevis* oocytes were purchased from Ecocyte (Dallas, TX). A Drummond Nanoject III was used to inject 40 nL of cDNA coding for $\alpha 5$, $\beta 3$, and $\gamma 2$ subunits in a 1:1:10 ratio, respectively, into each oocyte. Oocytes were stored in incubation medium (ND96 supplemented with 2 mM sodium pyruvate, 50 mg/mL gentamicin, and 10 mL of heat-inactivated HyClone horse serum [VWR, San Dimas, CA], adjusted to pH 7.5) in Petri dishes (VWR). All solutions were sterilized by passage through 0.22- μ m filters. Injected oocytes were stored at 18 °C for 48 h, then used in electrophysiology experiments up to 1 wk after injection. All chemicals used were reagent grade and purchased from Sigma-Aldrich. GABA stock solutions were prepared from powder and diluted with modified Barth's solution (MBS) containing 88 mM NaCl, 1 mM KCl, 10 mM HEPES, 0.82 mM MgSO₄, 2.4 mM NaHCO₃, 0.91 mM CaCl₂, and 0.33 mM Ca(NO₃)₂, adjusted to pH 7.5 (17). BB stock solutions were prepared by dissolving powder forms with dimethyl sulfoxide (DMSO) and serially diluted with MBS (DMSO \leq 0.05%)



The right common carotid artery was cannulated for measurement of blood pressure and heart rate via a PE23 pressure transducer. The transducer was connected to an ADInstruments (Colorado Springs, CO) quad bridge and blood pressure was monitored continuously throughout the duration of the experiment through LabChart version8 (ADInstruments). Heart rate and blood pressure were quantified for each of the study groups when either BB (2.5, 5, 10, and 20 mg/kg), BB vehicle (5% Pharnasolve, 30% PEG, 3% ethanol, and 62% solutol in 30% water, pH 8.0), or propofol (0, 2.5, 5, and 10 mg/kg) were infused IV over 1 min through the right internal jugular vein. The blood pressure and heart rate effects of a given dose were recorded 3 min after initiation of the drug injection.

Data Analysis. High-throughput screening was performed using the Flexible Docking and CDocker algorithms within Discovery Studio 4.0 (Accelrys Inc., San Diego, CA), as well as with the Chemical Abstracts database for the search of commercially available structures. All in vivo analyses were conducted using Prism 6.0 (GraphPad Software, Inc., San Diego CA); for each data point, 5 animals were tested. Dose–response curves were analyzed using the regression method adapted from Waud et al. (36). Electrophysiology recordings were analyzed with Igor Pro Software (Wavemetrics, Portland, OR). Each graph was the result of 5 experiments to report average response at each and SDS.

1. E. J. Bertaccini, O. Yoluk, E. R. Lindahl, J. R. Trudell, Assessment of homology templates and an anesthetic binding site within the γ -aminobutyric acid receptor. *Anesthesiology* **119**, 1087–1095 (2013).
2. V. S. Fahrenbach, E. J. Bertaccini, Insights into receptor-based anesthetic pharmacophores and anesthetic-protein interactions. *Methods Enzymol.* **602**, 77–95 (2018).
3. A. Jenkins et al., Evidence for a common binding cavity for three general anesthetics within the GABAA receptor. *J. Neurosci.* **21**, RC136 (2001).
4. S. A. Forman, Clinical and molecular pharmacology of etomidate. *Anesthesiology* **114**, 695–707 (2011).
5. R. L. Wagner, P. F. White, P. B. Kan, M. H. Rosenthal, D. Feldman, Inhibition of adrenal steroidogenesis by the anesthetic etomidate. *N. Engl. J. Med.* **310**, 1415–1421 (1984).
6. B. Asproni et al., Synthesis, structure-activity relationships at the GABA(A) receptor in rat brain, and differential electrophysiological profile at the recombinant human GABA(A) receptor of a series of substituted 1,2-diphenylimidazoles. *J. Med. Chem.* **48**, 2638–2645 (2005).
7. J. F. Cotten et al., Carboetomidate: A pyrrole analog of etomidate designed not to suppress adrenocortical function. *Anesthesiology* **112**, 637–644 (2010).
8. M. P. Mascia et al., Ethyl 2-(4-bromophenyl)-1-(2,4-dichlorophenyl)-1H-4-imidazolecarboxylate is a novel positive modulator of GABAA receptors. *Eur. J. Pharmacol.* **516**, 204–211 (2005).
9. S. Shanmugasundararaj et al., Carboetomidate: An analog of etomidate that interacts weakly with 11 β -hydroxylase. *Anesth. Analg.* **116**, 1249–1256 (2013).
10. P. J. Lein, C. D. Barnhart, I. N. Pessah, Acute hippocampal slice preparation and hippocampal slice cultures. *Methods Mol. Biol.* **758**, 115–134 (2011).
11. M. C. Bieda, H. Su, M. B. Maciver, Anesthetics discriminate between tonic and phasic γ -aminobutyric acid receptors on hippocampal CA1 neurons. *Anesth. Analg.* **108**, 484–490 (2009).
12. M. B. Maciver, Anesthetic agent-specific effects on synaptic inhibition. *Anesth. Analg.* **119**, 558–569 (2014).
13. J. A. Gredell, P. A. Turnquist, M. B. Maciver, R. A. Pearce, Determination of diffusion and partition coefficients of propofol in rat brain tissue: Implications for studies of drug action in vitro. *Br. J. Anaesth.* **93**, 810–817 (2004).
14. R. A. Pearce, Physiological evidence for two distinct GABAA responses in rat hippocampus. *Neuron* **10**, 189–200 (1993).
15. M. Vargas-Caballero, L. J. Martin, M. W. Salter, B. A. Orser, O. Paulsen, alpha5 subunit-containing GABA(A) receptors mediate a slowly decaying inhibitory synaptic current in CA1 pyramidal neurons following Schaffer collateral activation. *Neuropharmacology* **58**, 668–675 (2010).
16. R. P. Bonin, L. J. Martin, J. F. MacDonald, B. A. Orser, Alpha5GABAA receptors regulate the intrinsic excitability of mouse hippocampal pyramidal neurons. *J. Neurophysiol.* **98**, 2244–2254 (2007).
17. H. T. Nguyen et al., Behavior and cellular evidence for propofol-induced hypnosis involving brain glycine receptors. *Anesthesiology* **110**, 326–332 (2009).
18. B. Wang et al., An etomidate analogue with less adrenocortical suppression, stable hemodynamics, and improved behavioral recovery in rats. *Anesth. Analg.* **125**, 442–450 (2017).
19. F. de Wit et al., The effect of propofol on haemodynamics: Cardiac output, venous return, mean systemic filling pressure, and vascular resistances. *Br. J. Anaesth.* **116**, 784–789 (2016).
20. M. P. Mascia et al., Differential modulation of GABA(A) receptor function by aryl pyrazoles. *Eur. J. Pharmacol.* **733**, 1–6 (2014).
21. S. A. Forman, Molecular approaches to improving general anesthetics. *Anesthesiol. Clin.* **28**, 761–771 (2010).
22. D. E. Raines, The pharmacology of etomidate and etomidate derivatives. *Int. Anesthesiol. Clin.* **53**, 63–75 (2015).
23. J. Koska et al., Fully automated molecular mechanics based induced fit protein-ligand docking method. *J. Chem. Inf. Model.* **48**, 1965–1973 (2008).
24. H. M. Berman et al., The protein data bank. *Nucleic Acids Res.* **28**, 235–242 (2000).
25. H. Braberg et al., SALIGN: A web server for alignment of multiple protein sequences and structures. *Bioinformatics* **28**, 2072–2073 (2012).
26. S. F. Altschul et al., Gapped BLAST and PSI-BLAST: A new generation of protein database search programs. *Nucleic Acids Res.* **25**, 3389–3402 (1997).
27. D. G. Higgins, J. D. Thompson, T. J. Gibson, Using CLUSTAL for multiple sequence alignments. *Methods Enzymol.* **266**, 383–402 (1996).
28. N. Eswar, D. Eramian, B. Webb, M. Y. Shen, A. Sali, Protein structure modeling with MODELLER. *Methods Mol. Biol.* **426**, 145–159 (2008).
29. E. J. Bertaccini, J. R. Trudell, E. Lindahl, Normal-mode analysis of the glycine alpha1 receptor by three separate methods. *J. Chem. Inf. Model.* **47**, 1572–1579 (2007).
30. B. Delley, Dmol, a standard tool for density functional calculations: Review and advances. *Theor. Comput. Chem.* **2**, 221–254 (1995).
31. B. R. Brooks et al., CHARMM: The biomolecular simulation program. *J. Comput. Chem.* **30**, 1545–1614 (2009).
32. A. Naito et al., Glycine and GABA(A) ultra-sensitive ethanol receptors as novel tools for alcohol and brain research. *Mol. Pharmacol.* **86**, 635–646 (2014).
33. D. I. Perkins et al., Loop 2 structure in glycine and GABA(A) receptors plays a key role in determining ethanol sensitivity. *J. Biol. Chem.* **284**, 27304–27314 (2009).
34. B. A. Dagne et al., High dose gamma radiation selectively reduces GABAA-slow inhibition. *Cureus* **9**, e1076 (2017).
35. P. Hoerbelt, B. D. Heifets, “Native system and cultured cell electrophysiology for investigating anesthetic mechanisms” in *Methods in Enzymology*, R. G. Eckenhoof, I. J. Dmochowski, Eds. (Academic Press, 2018), pp. 301–338.
36. D. R. Waud, On biological assays involving quantal responses. *J. Pharmacol. Exp. Ther.* **183**, 577–607 (1972).